Thruster Allocation and Mapping of Aerial and Aquatic Modes for a Morphable Multimodal Quadrotor

Yu Herng Tan and Ben M. Chen, *Fellow, IEEE*

***Abstract*—Although there have been several proposed methods and existing prototypes demonstrating the functionality of aerial–aquatic vehicles, most are fundamentally aerial vehicles with varying degrees of operability when submerged. We aim to improve the balance of aerial–aquatic functionality by proposing a morphable vehicle structure, where the rotors can be tilted to allow thrust vectoring when underwater. Here, in this article, we present a revised prototype implementing the idea and define the details of the aerial and aquatic modes as they are distinctly different from any existing configurations and require unique RC input to actuator output mappings. Based on the first principles model derived from the vehicle structure, we developed an appropriate thruster allocation and mapping system that will allow a single user to control the vehicle manually in both aerial and aquatic modes.**

***Index Terms*—Aquatic robots, mobile robots, unmanned aerial vehicles.**

I. Introduction

AERIAL–aquatic robots are multimodal robots that are able to operate in both air and water. Besides being able to function across greater terrain as compared to standard single mode robots, these multimodal robots also avoid the need for interrobot communication and coordination that is necessary for a multimodal heterogeneous robot team that performs similar functions. However, the challenges faced by these robots include having to deal with divergent environmental properties in different mediums, which makes their design difficult to optimise or even just to achieve basic functionality and efficiency. In particular, aerial–aquatic robots have to navigate the 3-D fluid spaces of air and water, which are fundamentally different due to the respective fluid densities. As water is almost a thousand times denser than air, a significant buoyancy force related to the vehicle's volume will be present when submerged. In both mediums, a fundamental requirement is to overcome the static forces, such as gravity and buoyancy; hence, the basic design aim in air, to minimize weight, is distinctly different from that in water, which is to achieve neutral buoyancy. For a fixed volume, these two requirements would be contradictory as being lightweight implies low density, which can lead to excessive buoyancy that is undesirable. Furthermore, the different viscosity and conductivity of air and water also pose challenges individually to the aspects of propulsion, control, and communication of the vehicle, causing many well-established aerial solutions, such as radio communication and localization methods to be ineffective underwater. On the other hand, alternatives developed for aquatic operation, such as acoustic communication and navigation, are often large and bulky, making them unsuitable for aerial usage. These further complicate design considerations when they have to be combined in a single hybrid vehicle.

Although there are several examples and working prototypes pursuing the idea of aerial–aquatic operation, there has yet to be a common consensus on the best design approach for such a robot. Due to the relatively more demanding nature of aerial flight, most existing platforms, such as those presented in [1]–[5], are fundamentally aerial vehicles with limited capabilities or compromised efficiency in water. However, to achieve the full potential of this concept, it is necessary to consider both operating regimes during the design phase as balanced aerial and aquatic functionality would be the ultimate aim.

With the widely varying requirements across the two mediums, it is intuitive to use a morphable design that allows a single vehicle to adapt to its current medium requirements. As compared to existing aerial–aquatic robots, most of which have identical hardware structures to either fixed wing or multirotor aircraft, we proposed a concept in [6], which aims to adapt a multirotor by using a morphable structure to provide more flexibility in thruster orientation and hence resulting in vehicle functionality that is more balanced in both mediums instead of being primarily aerial. The morphable structure consists of a symmetrically linked tilt mechanism that rotates each thruster about its arm axis. This action of thrust vectoring, together with the four thruster layout, allows the thrust components to act in the direction that is needed in each medium: vertically in air, and

Manuscript received January 8, 2020; revised March 24, 2020; accepted April 24, 2020. Date of publication May 28, 2020; date of current version August 13, 2020. The work of Ben M. Chen is supported in part by the Key Program of the National Natural Science Foundation of China under Grant U1613225, and in part by Peng Cheng Laboratory. Recommended by Technical Editor Q. Xu and Senior Editor X. Chen. *(Corresponding author: Yu Herng Tan.)*

Yu Herng Tan is with the Department of Electrical and Computer Engineering, National University of Singapore, Singapore (e-mail: herng@u.nus.edu).

Ben M. Chen is with the Department of Electrical and Computer Engineering, National University of Singapore, Singapore, and also with the Department of Mechanical and Automation Engineering, Chinese University of Hong Kong, Hong Kong (e-mail: bmchen@cuhk.edu.hk).

Color versions of one or more of the figures in this article are available online at https://ieeexplore.ieee.org.

Digital Object Identifier 10.1109/TMECH.2020.2998329

1083-4435 © 2020 IEEE. Personal use is permitted, but republication/redistribution requires IEEE permission.
See https://www.ieee.org/publications/rights/index.html for more information.

Authorized licensed use limited to: National Univ of Defense Tech. Downloaded on February 24,2025 at 15:21:25 UTC from IEEE Xplore. Restrictions apply.

primarily in the lateral plane for horizontal movement in water. While existing aeria–aquatic multirotors commonly have to pitch and roll at large angles to effectively move underwater, the proposed concept avoids this by tilting the thrusters instead. This is useful for further extensions such as vision-based localization as the attachment and orientation of cameras or other sensors would not be affected by large body rotations.

In this article, we present the second generation prototype of the mechanism proposed in [6] in addition to defining the operational modes in both air and water, which were previously undefined. The main contribution includes defining the thruster allocation and mapping to the input channels and showing how this relates to the translational and rotational motions. With the addition of the thrust vectoring mechanism, the vehicle has five output channels instead of the usual four of a quadrotor. This is further complicated by the fact that the tilt angle alters the direction and hence component of rotational and translational acceleration that the thruster is producing. Based on the first principles model of the vehicle, the radio control (RC) transmitter input to thruster output allocations are designed such that a single human user can intuitively operate the vehicle in its various modes.

The rest of this article is organized as follows. Existing solutions and aerial–aquatic prototypes are summarized in Section II, where we identify the limitations of common solutions. Next, we introduce the updated prototype and hardware design in Section III and the model of the vehicle is given in Section IV. Using this model, the thruster mappings for the aerial and aquatic modes are defined in Section V and the implementation of the proposed mappings on the actual prototype is shown in Section VI. Finally, Section VII concludes this article.

II. Background

In an early survey of aerial–aquatic vehicles, Yang *et al.* [7] identified the simplest type of aerial–aquatic vehicles as *seaplane-type* vehicles which can land on and take-off from the water surface but do not perform any submerged movement. While such definitions have applications in water sampling [8] or can be used to extend the endurance of vehicles through lake-hopping [9] and sailing [10], there remains wider possibilities and applications for vehicles with greater underwater function.

Besides the aforementioned challenges posed by the differences in air and water as fluid mediums, the greatest difficulty in the design of any aerial–aquatic hybrid vehicle is the fact that the aerial demands of minimizing weight while generating sufficient lift typically limits the form and payload of a vehicle. Using separate propulsion systems integrated into a single vehicle implies that the aquatic system is effectively dead weight that has to be carried in the aerial phase while complex adaptive mechanisms would also incur a large weight penalty. As such, aerial–aquatic vehicles often take the form of common aerial platforms such as fixed wing planes or multirotors.

The fixed wing platform has been adapted for hybrid use in the prototypes presented in [1], [4], [11], [12], and is popular due to its endurance and range capabilities in air. These prototypes operate aquatically in a similar way to aerial flight, commonly using the same propeller and control surfaces, and are capable of high speed cruise flight when in the air. These existing examples demonstrate several different ways in which a general fixed wing platform can be adapted for aquatic use: [1] features floodable wing compartments to obtain the desired buoyancy when submerged; [4] adds a separate aquatic propeller; and [11] uses retractable wings to minimize drag and impact force upon water entry.

Alternatively, multirotors have also been adapted for hybrid usage. While the Naviator [13], with an X8 configuration, moves underwater using similar roll, pitch, and yaw movement as aerial operation, the Looncopter [5] uses an active buoyancy control system to tilt its entire body axes such that the thrusters are acting in the horizontal plane. Further hybrid possibilities have also been demonstrated by combining multiple operation modes, such as the NEZHA [14], where a standard quadrotor is combined with tailsitter capabilities in air and underwater glider function in water.

Transitioning from the aerial to underwater phase is relatively straightforward regardless of the vehicle design as the vehicle can simply land, drop or dive into the target water body. On the other hand, the transition from aquatic to aerial phase is less direct as it involves breaking the water surface, water shedding, and for propeller-driven vehicles the transition from low revolutions per minute (RPM) to high RPM operation. As a key point in the vehicle's mission profile, this transition phase has been well studied and evaluated. For fixed wing type platforms, the disadvantage of a water surface runway take-off has been overcome through the use of alternative water exit methods such as water jet launch [11] or vertical exit [1], [4], while an angled water exit from a submerged position has also been shown to be feasible in [12] at the right body angles. For multirotors, an X8 layout [3], [13] ensures that either the top or bottom set of four thrusters are in the same medium and hence can maintain the vehicle's attitude and provide consistent thrust at any stage during the transition out of water. A simpler solution, though susceptible to disturbances in the water, is to allow the multirotor to float with its propellers above the water surface before directly taking off. Furthermore, it has also been shown in [15] that direct water exit is also possible even with the most basic quadrotor configurations. With the multirotor attitude stabilized through feedback, all the thrusters can simultaneously transition from water to air and take-off.

While the above examples show that there are many possibilities in the design for these hybrid vehicles, many of the existing solutions still use identical hardware configurations in both air and water. With the difference in medium requirements, this implies that the vehicle is likely to be suboptimal in either one or both of its operating modes. To improve this, the use of a morphable structure can reduce the mismatch and align the vehicle closer to the optimal configuration in both mediums, as long as it is sufficiently lightweight to avoid compromising aerial performance. Examples of these include retractable wings [11] to reduce the impact upon hitting the water and a flooded wing component to reduce buoyancy [1], [4]. However, these examples still only produce passive effects as the thrusters and actuators operate under the same principles as in aerial

Authorized licensed use limited to: National Univ of Defense Tech. Downloaded on February 24,2025 at 15:21:25 UTC from IEEE Xplore. Restrictions apply.

flight. Even though the medium change will affect the fluid dynamics of the vehicle, the structure of the first principles model is mostly similar to that in air. As such, there is often no explicit distinction between the operation in the two mediums from a vehicle propulsion output perspective. This limits the effectiveness of the vehicle's design, as there is no solution to converting the primary need of generating lift in air to obtaining neutral buoyancy and multidirectional thrusting in water.

With its ability to hover and the ease of direct water-to-air transition without the need for external devices, we chose the multirotor platform as a basis for our design. Instead of using a fixed hardware configuration, we propose a mechanism that will allow the thrusters to tilt in water so that they act in the lateral plane, similar to the vectored thruster layouts common in remotely operated underwater vehicles. This rotation is further extended so that the thrusters can act vertically downward, effectively enabling bidirectional thrusting using the same set of fixed pitch propellers.

While the concept appears similar to existing tiltrotor vertical take-off and landing (VTOL) designs, the proposed design is unique from well-known examples such as the V-22 Osprey [16] and V-280 Valor [17] in both function and fundamental design. Instead of using the thrust vectoring for transitioning between vertical lift and forward cruise flight, it is used to adapt an aerial structure for aquatic use. As such, the design benefits from the versatility afforded by thrust vectoring, while avoiding the complex transition stages associated with tiltrotor operation in air as the tilting is only activated in water, where the vehicle dynamics are inherently damped by the high fluid density and the presence of buoyancy is able to counter some or all of the weight. In addition, the thrust vectoring mechanisms for all four thrusters of the quadrotor are designed to be coupled and symmetric. As compared to modern tailsitter designs [18], which provide individual vectoring control of each thruster as an additional control input, linking the thrust vectoring mechanism into a single unit is both possible and preferred here due the demands of the intended application. Unconventional aerial platforms, such as the THOR [19], which uses thrust vectoring to morph between fixed-wing hover mode and rotary wing operation, demonstrate a similar idea of using thrust vectoring to alter the operating mode of a single platform, though there is as yet no existing example that uses this concept for adapting between two different fluid mediums. Linking the thrust vectoring mechanism also allows a working design to be achieved with minimal complexity. As such the proposed mechanism, which is described in detail in Section III, is mechanically simple and can be built on a small scale, unlike classical tiltrotors which are historically associated with being large and complex.

In the same way that tiltrotor VTOLs and tailsitters differ from standard fixed wing planes, the proposed configuration is significantly different from standard multirotors whenever the thrust vectoring mechanism is activated. As such, there is a need to break down the implications of the design and the necessary thruster allocations to make the proposed design functional as the operational functions of the aquatic mode is unlike any existing platform. The details of the proposed design are described in Sections III and IV.

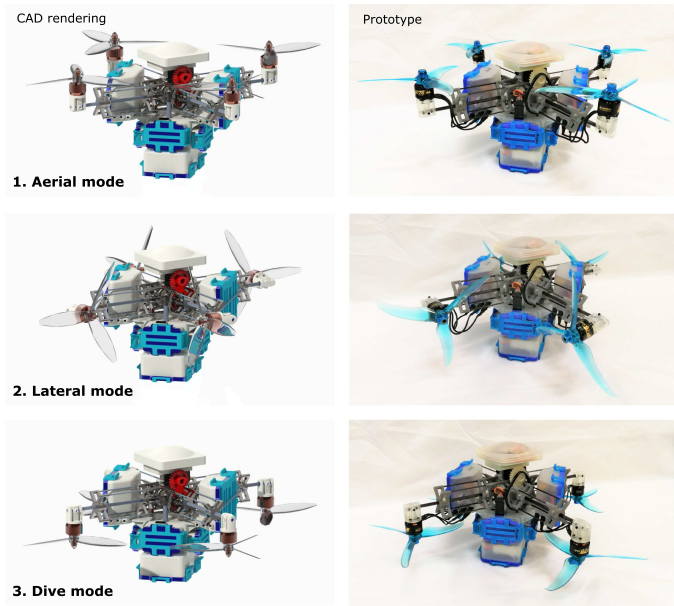

Fig. 1. CAD rendering (L) and the current prototype (R) of the proposed morphable aerial–aquatic quadrotor showing the rotors tilted at various angles and configurations.

III. Proposed Design

The fully assembled prototype is shown in Fig. 1 and an exploded view is shown in Fig. 2. Weighing 559.4 g with a motor-to-motor wheelbase of 250 mm, the proposed design revolves around the core tilt mechanism that controls the thrust vectoring, which has been introduced in our earlier work [6]. This core mechanism links the four arms of the quadrotor through four mitre gears at the center of the vehicle, allowing coupled symmetric tilting of all four rotors about their respective arm axes where the tilt angle is equal for each arm. This is activated through a single servo actuator which drives one of the arm rods through a transmission gear, allowing the morphing mechanism to be simple and lightweight.

As compared to the initial concept prototype in [6], the current prototype presented here has been significantly revamped and features a different structural design that has been further optimized for aquatic operation. The structure of the core frame, which houses the core mechanism, was redesigned to be structurally stiffer and more compact. The entire core frame and mechanism weighs 110 g excluding the motors, which is comparable to a standard frame structure of a similar size. Another major improvement is the waterproofed hull with complex geometry that is designed according to the desired static stability and volume distribution, as opposed to the initial prototype in [6] that features a simple cylindrical hull.

Several aspects of the prototype design are tailored for the proposed hybrid operation. The thrust vectoring mechanism allows the vehicle to reduce the impact of increased fluid resistance in water as it rotates only its thrusters instead of the entire vehicle body, which is the case for existing aerial-aquatic prototypes with fixed thruster layouts [3], [5]. Through adjusting

Authorized licensed use limited to: National Univ of Defense Tech. Downloaded on February 24,2025 at 15:21:25 UTC from IEEE Xplore. Restrictions apply.

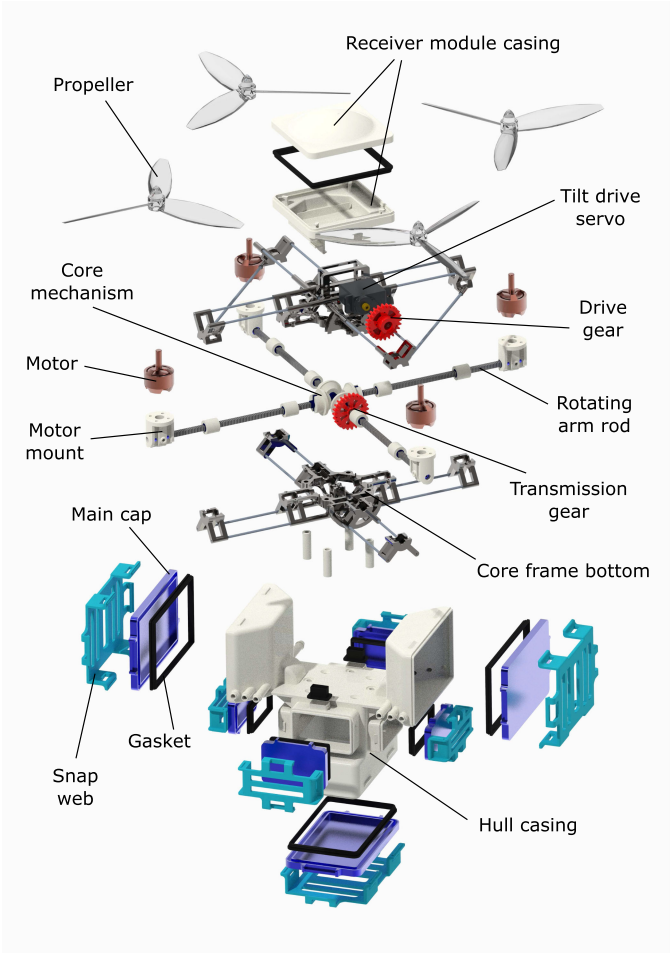

Fig. 2. Exploded rendering of the current prototype.

the direction of the thrusters, a larger component of the thrust can be directed in the direction of motion instead of relying on rotation of the body to direct a component of the thrust in the lateral directions. In addition, minimizing the footprint of the vehicle and size of the hull will generally reduce the fluid resistance of the body, which is done here by component arrangement and compact packaging.

The improved hull assembly consists of the hull casing and the snap caps that seal the openings of the hull casing. The volume distribution of the hull, which determines the vehicle's centre of buoyancy (COB), together with the placement of the components to determine the weight distribution and center of gravity (COG), was designed iteratively to achieve the desired positions and margins between these two key points. As a safety feature, the vehicle is designed to be slightly buoyant so that when radio link is lost, the throttle is cut and the vehicle can float to the surface. Two sidepods that extend into the sides of the core frame allow the volume distribution to be shifted upward, as the COB needs to be vertically above the COG for static stability. These sidepods house the electronic speed controllers (ESCs) as they are relatively lightweight and can be positioned close to the motors here. The power distribution board (PDB) is mounted within the hull casing directly under the core mechanism, with the flight controller stacked beneath it using nylon spacers. Last, the battery is housed at the bottom of the hull below the avionics. The hull casing is 3-D printed as a single component using stereolithography (SLA), with openings designed around the components such as the battery compartment and access to the flight controller for firmware and parameter adjustments. To maintain the symmetry of the hull, there are openings on each of the four sides of the flight controller, each outward facing side of the sidepods, and the bottom of the hull where the battery is located.

The snap caps that seal these openings are subassemblies themselves, consisting of the main cap, gasket, and snap web. These are 3-D printed using different materials in order to achieve the desired waterproof seal. The gasket, which fills the gap between the hull opening and the main cap, is 3-D printed using fused deposition modeling (FDM) with thermoplastic polyurethane (TPU). This material allows the gasket and hence opening to be customized as needed through FDM, while also providing sufficient flexibility to be a functional gasket. The main cap, which holds the gasket, is made from PLA material using FDM. This provides higher rigidity as compared to SLA materials, which is crucial in maintaining the shape of the opening to ensure a good seal. To lock the main cap in place and press the gasket tightly against the opening, the snap web wraps around the main cap and latches onto extrusions on the hull casing. This piece is printed using SLA, which is durable enough to withstand repeated latching and release, and is designed as a *web* to minimize weight as it does not need to be structurally rigid. Designing the snap caps as an assembly of these three parts allows different materials to be used as needed, and they can all be easily manufactured at low costs using desktop printers.

$$\mathbf{F_b} = \begin{bmatrix} \frac{\sqrt{2}}{2}\cos\beta(|T_1| - |T_2| + |T_3| - |T_4|) \\ \frac{\sqrt{2}}{2}\cos\beta(-|T_1| + |T_2| + |T_3| - |T_4|) \\ \sin\beta(|T_1| + |T_2| + |T_3| + |T_4|) \end{bmatrix} \tag{1}$$

$$+ (mg - U)\begin{bmatrix} -\sin\theta \\ \sin\phi\cos\theta \\ \cos\phi\cos\theta \end{bmatrix} \tag{2}$$

$$\mathbf{M_b} = \begin{bmatrix} \frac{l}{\sqrt{2}}\sin\beta\,(-|T_1| + |T_2| + |T_3| - |T_4|) \\ \frac{l}{\sqrt{2}}\sin\beta\,(|T_1| - |T_2| + |T_3| - |T_4|) \\ l\cos\beta(|T_1| + |T_2| - |T_3| - |T_4|) \end{bmatrix} \tag{3}$$

$$+ z_t \begin{bmatrix} -\frac{\sqrt{2}}{2}\cos\beta(-|T_1| + |T_2| + |T_3| - |T_4|) \\ -\frac{\sqrt{2}}{2}\cos\beta(|T_1| - |T_2| + |T_3| - |T_4|) \\ 0 \end{bmatrix}$$

$$+ \sum_i^4 \begin{bmatrix} M_{iX} \\ M_{iY} \\ M_{iZ} \end{bmatrix}. \tag{4}$$

The receiver and pulse position modulation (PPM) encoder are housed separately in their own sealed module that is attached to the top of the core mechanism. This allows the receiver to be well clear of any interference from the other avionics. A signal wire is passed through, from this receiver module to the main hull, where the flight controller is.

Authorized licensed use limited to: National Univ of Defense Tech. Downloaded on February 24,2025 at 15:21:25 UTC from IEEE Xplore. Restrictions apply.

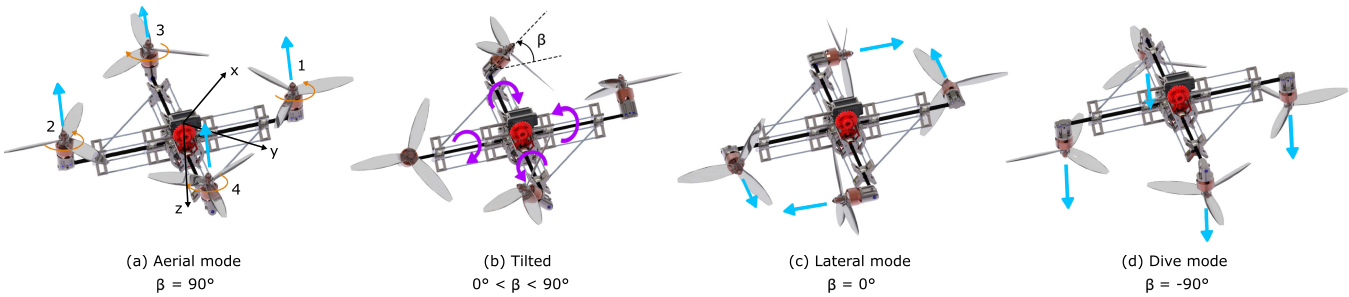

Fig. 3. Schematic diagram showing the axes convention and motor labeling used, as well as the different configurations possible with various values of the tilt angle β.

IV. Vehicle Model

The first principles model of the vehicle can be derived according to the vehicle and mechanism structure to understand the effects of the thrust vectoring as implemented in the proposed design. Here, we will use the standard North–East–Down local coordinates to indicate the axes direction of the body frame, where the origin is the COG of the vehicle. The orientation of the body axes in the global frame is defined by the Euler angles $\mathbf{\Theta} = [\phi, \theta, \psi]^{\mathrm{T}}$. The body frame definition, thruster layout, and numbering used in the model below follow those shown in Fig. 3.

With the tiltable configuration, the vehicle now has an additional input variable of the tilt mechanism setting that determines the tilt angle, β. The definition and value range of the angle β is visually represented in Fig. 3. The physical design limits $-\pi/2 \leq \beta \leq \pi/2$, as the volume space associated with the remaining rotation angles are taken up by the hull sidepods and structural support of the core frame. Nevertheless, $-\pi/2 \leq \beta \leq \pi/2$ is sufficient to allow full actuation of the vehicle. As the mechanical link of the tilt mechanism uses a 1:1 gear ratio, the tilt angle of each rotor will be the same, although the direction will depend on the arm axes as shown in Fig. 3. Here, we define the tilt angle such that $\beta = \pi/2$ corresponds to the standard aerial mode, $\beta = 0$ to the full lateral mode, and $\beta = -\pi/2$ to the vertical dive mode as shown in Fig. 3.

A. Vectored Thrust Components

With the introduction of the tilt angle, the vectored thrust of the ith thruster T_i can be broken into the vertical and lateral components $T_{i,\text{vert}}$ and $T_{i,\text{lat}}$, respectively. According to the geometry of the design

$$T_{i,\text{vert}} = |T_i| \sin\beta \tag{5}$$

$$T_{i,\text{lat}} = |T_i| \cos\beta \tag{6}$$

$T_{i,\text{lat}}$ can be further broken down into components that align with the local body axes, where $T_{i,x} = T_{i,y} = \frac{\sqrt{2}}{2} T_{i,\text{lat}}$. With $T_{i,z} = T_{i,\text{vert}}$, the vectored thrust components of the ith motor in the local body axes can be written as follows:

$$\mathbf{T_i} = \begin{bmatrix} a \times \frac{\sqrt{2}}{2} |T_i| \cos\beta \\ b \times \frac{\sqrt{2}}{2} |T_i| \cos\beta \\ |T_i| \sin\beta \end{bmatrix} \tag{7}$$

where a, b are scalars according to the direction of the motor

$$a = \begin{cases} 1, & \text{if } i = 1,3 \\ -1, & \text{if } i = 2,4 \end{cases} \quad b = \begin{cases} 1, & \text{if } i = 2,3 \\ -1, & \text{if } i = 1,4 \end{cases}. \tag{8}$$

The presence of the $T_{i,\text{lat}}$ component also results in an additional moment if the thrusting force is not vertically aligned with the COG, which is the case here due to the need for a low COG to obtain the desired static stability. While the $T_{i,\text{vert}}$ component creates a moment about the x- and y-axes with a moment arm of $\frac{l}{\sqrt{2}}$, where l is the half wheelbase of the vehicle, the moment arm of $T_{i,\text{lat}}$ is given by the vertical distance between the thrusting force and the COG, z_t. Therefore the moment vector produced by the ith motor can be written as follows:

$$\mathbf{M_i} = \begin{bmatrix} bl \times \frac{\sqrt{2}}{2} T_{i,z} - z_t T_{i,y} \\ al \times \frac{\sqrt{2}}{2} T_{i,z} - z_t T_{i,x} \\ cl \times T_{i,\text{lat}} \end{bmatrix} + \begin{bmatrix} M_{iX} \\ M_{iY} \\ M_{iZ} \end{bmatrix} \tag{9}$$

where M_{iX}, M_{iY}, M_{iZ} represent the moment in the X, Y, Z axis caused by the rotation of the ith motor, respectively, and c is the direction scalar for the yaw axis

$$c = \begin{cases} 1, & \text{if } i = 3,4 \\ -1, & \text{if } i = 1,2 \end{cases}. \tag{10}$$

B. First Principles Model

The force and moments in the proposed configuration can then be written as (2) and (4), where mg is the weight of the vehicle and U is the buoyancy force. Considering the relatively low rotational speeds of the motors in water, the moment component contributed by M_{iX}, M_{iY}, M_{iZ} are likely to be small and negligible.

The formulation above shows that the addition of the tilt angle variable allows direct actuation in all six translational and rotational directions of the vehicle. Although the system appears highly coupled and complex, it can be greatly simplified at certain values of β. First, at $\beta = \pi/2$ and $\beta = -\pi/2$, which correspond to the aerial [see Fig. 3(a)] and dive mode [Fig. 3(d)] respectively, $T_{i,\text{lat}} = 0$ and the thrusters act only in the vertical direction. As such, the second term in (4) will be zero and the thrusters only affect the three rotational moments and vertical translation.

Authorized licensed use limited to: National Univ of Defense Tech. Downloaded on February 24,2025 at 15:21:25 UTC from IEEE Xplore. Restrictions apply.

In the aerial mode, where $\beta = \pi/2$ and since $U = 0$ in air, (2) and (4) reduce to the model of a regular quadrotor

$$\mathbf{F_b} = \begin{bmatrix} 0 \\ 0 \\ |T_1| + |T_2| + |T_3| + |T_4| \end{bmatrix} + \text{mg} \begin{bmatrix} -\sin\theta \\ \sin\phi\cos\theta \\ \cos\phi\cos\theta \end{bmatrix} \quad (9)$$

$$\mathbf{M_b} = \begin{bmatrix} \frac{l}{\sqrt{2}}\left(-|T_1| + |T_2| + |T_3| - |T_4|\right) \\ \frac{l}{\sqrt{2}}\left(|T_1| - |T_2| + |T_3| - |T_4|\right) \\ M_1 + M_2 - M_3 - M_4 \end{bmatrix}. \quad (10)$$

Similarly, the vertical dive mode is simply the directional opposite of (9) and (10) in the heave, roll, and pitch components.

Although $\beta = 0$ corresponds intuitively with the actuators being directed in the lateral plane, this configuration will still generate a moment in pitch and roll due to the presence of the z_t term in (4). However, pure lateral movement is still possible at the value of $\beta = \beta^*$, where the first and second term of (4) cancel each other. As the thruster plane is elevated from the rotating arm, based on the dimensions of the physical prototype, the distance z_t varies with β according to the relationship

$$z_t = 0.036 + 0.028 \sin\beta. \quad (11)$$

With the value of $l = 0.125$ mm, the point where the two moment terms cancel, or the compensated lateral mode, will occur at $\beta^* = 0.354$ rad, or about 20.2°.

V. Aerial and Aquatic Mode Switching

As the morphable function of the proposed design requires distinctively different aerial and aquatic operation from the actuator outputs, these have to be defined in the flight controller firmware in order to be implemented. Here, one of the transmitter switches is used as the mode switch to set the vehicle in either aerial or aquatic mode. In this section, we will describe the actuator mappings of the hybrid operation, in particular the aquatic mode as mixing of the input channels is necessary to provide an intuitive user control interface with the addition of the extra tilt angle variable. It should be noted that even though both input and output channels use the same numerical numbering, they do not correspond directly to each other. The relationship is governed by the thruster mapping and mixer definition described below.

A. Hybrid Mode Channel Mapping

For purposes here, we will assume that the vehicle is statically stable and neutrally buoyant, therefore setting throttle as zero results in position holding. Even though the vehicle is in fact designed to be buoyant, this can be treated effectively as a fixed scalar offset from the described situation. The motion or action corresponding to each RC channel (CH) for the two modes are shown in Table I and the corresponding input channels on the RC transmitter are shown in Fig. 4.

In the proposed system, the aerial mode of the vehicle corresponds to the standard mapping of RC controls for a quadrotor (roll, pitch, throttle, yaw). Under manual (stabilized) control, these inputs are given by the four joysticks (CH1-4). In this mode, the tilt servo is not activated, i.e., fixed at $\beta = \pi/2$.

In the aquatic mode, the tilt angle becomes an active input and this results in the thruster outputs to have components acting in both rotational and translational acceleration depending on the tilt angle as defined in (2) and (4). As setting throttle to zero now effectively corresponds to a hover state due to the assumption of neutral buoyancy, the conventional throttle mapping has to be altered to take this into account in addition to the *bidirectional* thrusting made possible by the tilt mechanism. Furthermore, in the lateral configuration when $\beta = 0$, the thrusters components are directed in surge and sway as $T_{i,z} = 0$, hence they contribute primarily to linear acceleration instead of rotational acceleration. Similarly, in the compensated lateral configuration when $\beta = \beta^*$, the net acceleration produced act only in the directions of surge and sway when adjacent pairs of thrusters are activated (see Fig. 5). As the hardware configuration limits the use of at most two of the four thrusters when moving in a single direction in surge and sway, the RC joysticks CH1, CH2, and CH4 will have to correspond with selected actuation of the corresponding thrusters instead of all thrusters.

TABLE I
RC Channel Mappings for the Two Modes

CH	Aerial mode	Aquatic mode
1	ROLL	SWAY/ ROLL
2	PITCH	SURGE/ PITCH
3	THROTTLE	TILT×THROTTLE
4	YAW	YAW
5	MODE SWITCH	MODE SWITCH
6	-	CH3 THROTTLE LIMIT

Fig. 4. Futaba 7CHP transmitter used for the prototype.

B. Thruster Allocation for Aquatic Mode

In order to operate in the proposed configuration, separate allocation of thruster settings for lateral and vertical motion input is needed for manual control even though they are coupled at nonzero and nonperpendicular tilt angles. While a typical aerial thruster output ranging from 0 to 1 is given directly by the throttle joystick input, the throttle input here is divided into four components due to the need for selected actuation of the thrusters. These input channels correspond to the motor actuation as shown in

Authorized licensed use limited to: National Univ of Defense Tech. Downloaded on February 24,2025 at 15:21:25 UTC from IEEE Xplore. Restrictions apply.

TABLE II
MOTOR MAPPING AND THRUSTER VALUE ALLOCATION FOR EACH THRUSTER COMPONENT IN AQUATIC MODE

Input CH	Throttle component	Action	Max. value	+ input activated motors/ actuators	− input activated motors/ actuators
1	THR1	SWAY/ ROLL	0.3	2,3	1,4
2	THR2	SURGE/ PITCH	0.3	2,4	1,3
3	THR3	TILT×THROTTLE	0.3	$\beta^{\ddagger}$,1,2,3,4	$\beta^{\ddagger}$,1,2,3,4
4	THR4	YAW	0.1	1,2	3,4

‡The direction of the tilt angle β for positive and negative inputs are different and vary according to the curve shown in Fig. 7.

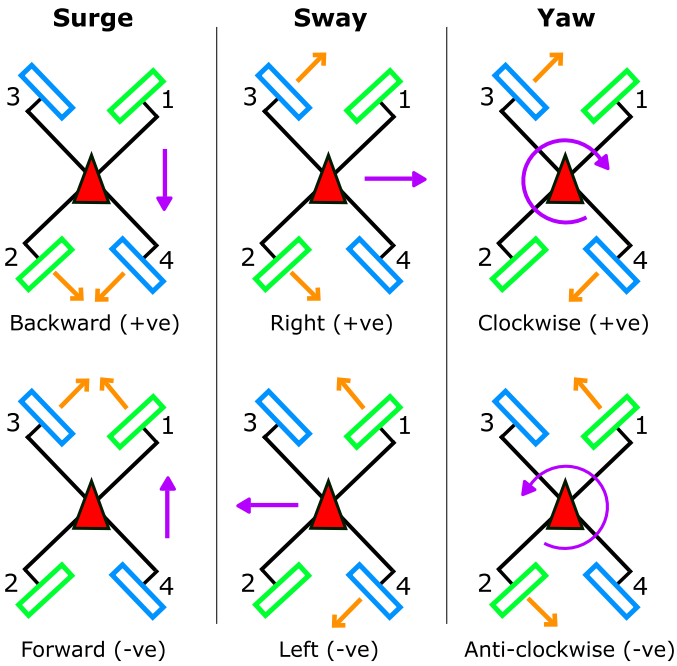

Fig. 5. Diagram showing the how inputs in lateral mode ($\beta = 0$) corresponds to the planar movement of the vehicle. The direction (+ve/−ve) indicated refers to the direction of the input that will activate the motors shown.

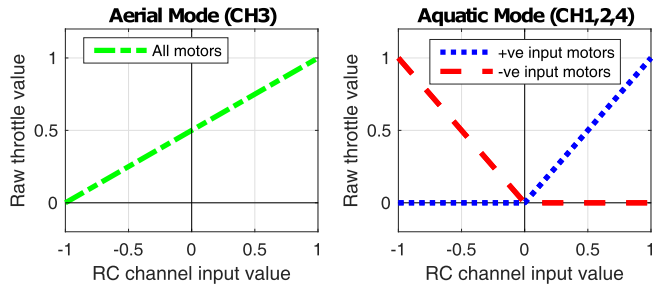

Fig. 6. Throttle curves for the aerial and aquatic modes differ in both the motors actuated and output mapping.

Table II, and the resulting vehicle movement is shown in Fig. 5. The throttle curves for the aquatic mode, as compared to the aerial mode, is shown in Fig. 6. Due to the thruster layout, it is necessary that the surge direction is mapped in the opposite direction (pushing CH2 backward giving a negative input value will map to forward movement) as at large positive β angles this actuation will result in rotational action and priority is given to intuitive control of the rotational movement to be consistent with aerial control.

Each joystick input sends an absolute value of the throttle component, with the input scaled to the maximum thruster component limit as shown in Table II, to the stated motors. The other motors receive a throttle component value of 0. The thruster output of each motor, $\mathrm{THR}_i, i \in \{1, 2, 3, 4\}$, is then simply the sum of the four thruster components for that motor

$$\mathrm{THR}_i = \mathrm{THR1}_i + \mathrm{THR2}_i + \mathrm{THR3}_i + \mathrm{THR4}_i. \quad (12)$$

This linear combination will allow the user to decouple the movement by actuating inputs in only one direction.

As the heave motion is reliant on the tilt mechanism for directional operation, the control requires the integrated operation of two RC inputs: the tilt angle and the throttle setting, as opposed to just the throttle setting in aerial mode. To allow feasible operation by a single user, the two channels will be mixed such that CH3 will control a function that includes both the tilt angle setting and throttle setting (TILT×THROTTLE), and an additional channel (dial/ CH6) will set the maximum throttle setting which the CH3 input will be scaled to. This allows the tilt action to be executed separately without throttle input from the TILT×THROTTLE channel by setting CH6 to zero, which will allow the vehicle to execute roll, pitch, and yaw movement in the aquatic mode. The mapping of the tilt servo is set as a linear variation with the joystick input of CH3, whereby the minimum joystick input (-1) corresponds to $\beta = \pi/2$ (motors pointing vertically upward) and the maximum input (+1) corresponds to $\beta = -\pi/2$ (motors pointing vertically downward). When CH6 is nonzero, this allows a positive CH3 input to execute a vertical dive ($\beta < 0$, identical outputs to all motors) and similarly a negative CH3 input to execute a vertical rise ($\beta > 0$). The direction is implemented as such to allow a smooth mode transition between the aerial and aquatic modes, as $\beta = \pi/2$ will correspond to the maximum negative position of the RC joystick in the aquatic mode, which also matches to the aerial tilt angle (fixed at $\beta = \pi/2$) with zero throttle in aerial mode, indicating standby for take-off.

As the thrust from a single thruster in the heave direction is given by $T_{i,z} = T_i \times \sin\beta$, and CH3 is the input of both β and T, if β is fixed as a linear function of CH3 then T can also be treated effectively as a function of β. Instead of setting T to be linear function of β, we can set $T = \sin\beta$, which will give a more desirable output function for $T_{i,z}$ as shown in Fig. 7.

VI. IMPLEMENTATION

A schematic of the avionics and actuator wiring is shown in Fig. 8. The flight controller used here is a Pixracer R15, which is sufficiently compact to be easily packaged within the waterproof hull. The four thrusters on actuator output channels

Authorized licensed use limited to: National Univ of Defense Tech. Downloaded on February 24,2025 at 15:21:25 UTC from IEEE Xplore. Restrictions apply.

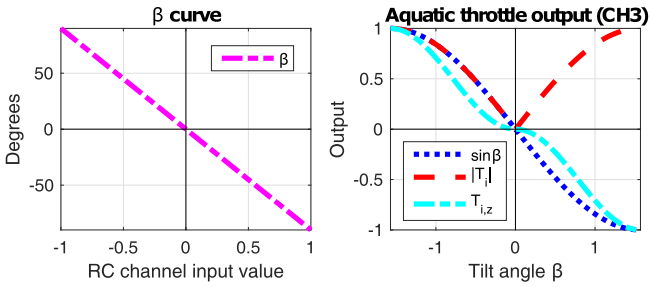

Fig. 7. Output curves associated with the mixed input CH3 that includes both the tilt angle β and thruster output.

1 to 4 are powered by T-MOTOR F20II-3700KV motors paired with T-MOTOR F35 A ESCs and the tilt servo is connected to actuator output channel 5. Manual control of the vehicle is achieved through a 35 MHz radio receiver linked to the operator transmitter, which is capable of operating in freshwater up to depths of 5 m. The receiver inputs are passed to the flight controller through a PPM encoder. A Holybro PM06 PDB provides power to the ESCs and servo rail of the Pixracer and the power source is a BOLT LiHV 3S 1000 mAh battery. As the same set of actuators and avionics are used for both aerial and aquatic operation, the only redundant component that has to be carried by the vehicle in either mode is the tilt servo when in flight. This accounts for 1.9% of the vehicle's all-up weight.

A. Firmware Implementation

To implement the thruster mapping described above, the flight controller firmware based on the PX4 flight stack [20] has to be modified in several ways. The basic structure and system flow of the PX4 firmware under manual control is shown in Fig. 9. The controller receives the RC inputs and generates the desired outputs, which are published to an actuator control group (ACG). The mixer then takes these ACG values, which may correspond to rotational setpoints, and converts them into actuator outputs that are sent as pulse width modulation (PWM) signals to the output servo rail.

As the two modes map to distinctly different output combinations, they will require different control regimes. As the mixer is fixed and loaded upon booting of the vehicle, the mode switching of the actuator outputs have to be implemented on a higher level of the control architecture. This modification was made in the controller block, where an additional check is made to verify if the mode switch position has changed. The mode is only switched when the transition conditions described in Section VI-B are fulfilled.

The aerial mode is identical to a standard quadrotor, and here the regular PX4 quadrotor control system is used. This controller outputs the various rate setpoints to ACG0, which corresponds to the roll, pitch, yaw, and thrust of the vehicle. However, the system also has to incorporate the underwater mode, which uses a direct passthrough of the RC controls scaled according to the weights defined in Section V-B. To do this, the aquatic mode will publish the scaled and summed outputs to a different ACG, ACG3, which is typically used for direct passthrough of RC signals.

Algorithm 1: Actuator Group Selection.

switch (current mode)
case aerial**:**
publish ACG3 $= 0$
run attitude control
generate attitude setpoint
publish rates to ACG0
case aquatic**:**
publish ACG0 $= 0$
generate scaled throttle components from RC passthrough
sum each throttle component to get $\text{THR}_i, i \in \{1, 2, 3, 4\}$
publish THR_i to ACG3
end switch

The mixer is a summation of ACG0 and ACG3, which correspond to the attitude control outputs and RC passthrough outputs, respectively. As such, it is necessary to set the unused ACG to zero. This procedure is summarized in Algorithm 1.

B. Transition Between Modes

To transition from aerial to aquatic mode, the vehicle simply lands on the water body and cuts the throttle. The transition to aquatic mode is only allowed when CH3 and CH6 are set to the minimum position and the other inputs are in their respective deadzones as described in Algorithm 2. Transition from the aquatic to aerial mode is similar, though we require an additional condition of the vehicle attitude being upright within a given margin to ensure that the vehicle can break the water evenly. As the current system is only tested under manual control, a low initial throttle setting is sufficient to balance the vehicle and ensure a clean water exit and transition to air. In future developments, an active controller will be designed to allow semiautonomous or autonomous transitions.

C. Experimental Testing

The prototype was tested in both aerial and aquatic conditions (see Fig. 10) and manual tests verified that the proposed system is functional and can be intuitively operated as intended. Aerial flight was tested by setting $\beta = \frac{\pi}{2}$ and operating like a standard quadrotor as described above. For aquatic tests, the lateral motions and vertical movement were tested to verify the regime above. In addition, vertical diving, and resurfacing was also tested by setting $\beta = -\frac{\pi}{2}$ and $\beta = \frac{\pi}{2}$, respectively. Entering the water from aerial flight is straightforward by landing directly on the water body. As the vehicle is buoyant, giving a positive CH3 and a nonzero CH6 input in aquatic mode will allow the vehicle to dive underwater.

Transition from water to air was similarly tested. After sitting at a standby floating position at the water surface, switching to aerial mode reactivates the attitude control of the vehicle. At this point, slowly increasing the throttle will allow the vehicle to

Authorized licensed use limited to: National Univ of Defense Tech. Downloaded on February 24,2025 at 15:21:25 UTC from IEEE Xplore. Restrictions apply.

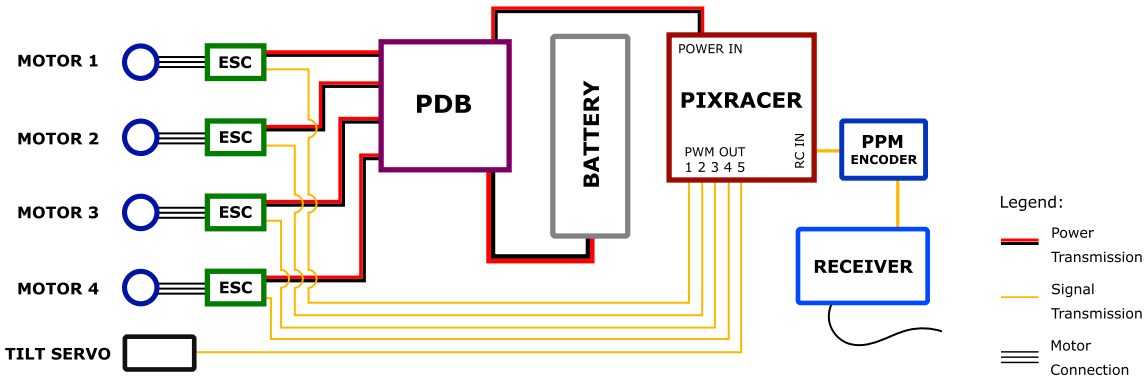

Fig. 8. Schematic diagram showing the connections between the avionics components and actuators.

Fig. 9. System flow of the PX4 firmware structure.

Algorithm 2: Transition Checks.

```
check mode switch position
if mode switch position not current mode then
  if CH3 and CH6 are in minimal position then
    if current mode is aquatic then
      {additional attitude check for aquatic to aerial
 transition}
      if attitude within upright stable margin then
        transition from aquatic to aerial mode
        update current mode
      else
        transition denied
      end if
    else
      transition from aerial to aquatic mode
      update current mode
    end if
  end if
else
  transition denied
end if
```

gradually increase the lift generated while stabilizing its attitude. Once all the propellers clear the water and enter air, the lift generation and flight continues as per a normal aerial quadrotor to complete the transition out of water. Besides the presence of skin friction resistance from water contact, which is negligible in this case due to the small external footprint of the vehicle as compared to its weight, the lift required for the vehicle to enter aerial flight from water is in fact similar to taking off from land. This is because at the floating point on the water surface, the buoyancy force is equal to the vehicle's weight, similar to how a stationary vehicle on land has a reaction force equal and

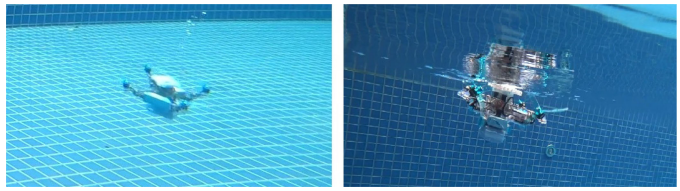

Fig. 10. Snapshots from the aquatic tests of the prototype.

opposite to its weight that is acting on it from the ground. As the lift generated increases, gradually lifting the vehicle out of the water, the volume that remains submerged decreases, resulting in a drop in the buoyancy force. If we consider a case of hovering at any point during this transition, where part of the vehicle body is still submerged, the sum of the current lift generated and buoyancy force will be equal to the vehicle's weight. This continues until the vehicle body is completely lifted out of the water, at which point hovering requires the total lift to be equal to its weight.

VII. Conclusion

In this article, we present the development of a morphable multimodal quadrotor, featuring a second generation prototype and detailing the thrust allocation and actuator mapping required to implement the proposed design. Based on the system model, the proposed allocation system was demonstrated to be functional and successfully incorporated the extra channel added under manual operation by a single user using a standard RC transmitter. Currently, the manual aquatic mode presented does not provide attitude feedback unlike standard aerial operation. Nevertheless, the system is still functional due to the large damping effect of movement in water caused by the high density and viscosity of the medium. Future work would include adding this aquatic attitude controller so that the intended advantage of the design, translational movement without extended rotation of the vehicle body, can be fully realized. In addition, a more thorough investigation of the hydrodynamics of the vehicle would improve both the functionality and future scalability of the design. To expand the work further, increasing the operational

Authorized licensed use limited to: National Univ of Defense Tech. Downloaded on February 24,2025 at 15:21:25 UTC from IEEE Xplore. Restrictions apply.

depth of the vehicle, which is currently limited by waterproofing and communication capabilities, should also be included as a design consideration. The versatility of the platform lends itself to different control strategies, which can be used to implement different movement functions in the aquatic mode, and the simple mechanical structure provides ample potential for future development.

References

[1] W. Weisler, W. Stewart, M. B. Anderson, K. J. Peters, A. Gopalarathnam, and M. Bryant, "Testing and characterization of a fixed wing cross-domain unmanned vehicle operating in aerial and underwater environments," *IEEE J. Ocean. Eng.*, vol. 43, no. 4, pp. 969–982, Oct. 2018.

[2] R. Siddall, A. Ortega Ancel, and M. Kovač, "Wind and water tunnel testing of a morphing aquatic micro air vehicle," *Interface Focus*, vol. 7, no. 1, 2017. [Online]. Available: http://rsfs.royalsocietypublishing.org/lookup/doi/10.1098/rsfs.2016.0085

[3] M. M. Maia, D. A. Mercado, and F. J. Diez, "Design and implementation of multirotor aerial-underwater vehicles with experimental results," in *Proc. IEEE/RSJ Int. Conf. Intell. Robots Syst.*, Sep. 2017, pp. 961–966

[4] W. Stewart *et al.*, "Design and demonstration of a seabird-inspired fixed-wing hybrid UAV-UUV system," *Bioinspiration Biomimetics*, vol. 13, no. 5, Aug. pp. 1–15, 2018.

[5] H. Alzu'bi, I. Mansour, and O. Rawashdeh, "Loon Copter: Implementation of a hybrid unmanned aquatic-aerial quadcopter with active buoyancy control," *J. Field Robot.*, vol. 35, no. 5, pp. 764–778, Aug. 2018.

[6] Y. H. Tan and B. M. Chen, "Design of a morphable multirotor aerial-aquatic vehicle," in *OCEANS MTS/IEEE Seattle*, pp. 1–8, Oct. 2019. [Online]. Available: https://ieeexplore.ieee.org/document/8962867/

[7] X. Yang, T. Wang, J. Liang, G. Yao, and M. Liu, "Survey on the novel hybrid aquatic aerial amphibious aircraft: Aquatic unmanned aerial vehicle (AquaUAV)," *Progr. Aerosp. Sci.*, vol. 74, pp. 131–151, Apr. 2015.

[8] P. Rodrigues *et al.*, "An open-source watertight unmanned aerial vehicle for water quality monitoring," in *OCEANS MTS/IEEE Washington*, pp. 1–6, Oct. 2015. [Online]. Available: http://ieeexplore.ieee.org/document/7404447/

[9] R.-A. Peloquin, D. Thibault, and A. L. Desbiens, "Design of a passive vertical takeoff and landing aquatic UAV," *IEEE Robot. Autom. Lett.*, vol. 2, no. 2, pp. 381–388, Apr. 2017.

[10] R. Zufferey *et al.*, "SailMAV: Design and implementation of a novel multi-modal flying sailing robot," *IEEE Robot. Autom. Lett.*, vol. 4, no. 3, pp. 2894–2901, Jul. 2019.

[11] R. Siddall and M. Kovac, "Fast aquatic escape with a jet thruster," *IEEE/ASME Trans. Mechatron.*, vol. 22, no. 1, pp. 217–226, Feb. 2017.

[12] J. Moore, A. Fein, and W. Setzler, "Design and analysis of a fixed-wing unmanned aerial-aquatic vehicle," in *Proc. IEEE Int. Conf. Robot. Autom.*, May 2018, pp. 1236–1243.

[13] M. M. Maia, P. Soni, and F. J. Diez-Garias, "Demonstration of an aerial and submersible vehicle capable of flight and underwater navigation with seamless air-water transition," to be published. [Online]. Available: https://arxiv.org/abs/1507.01932

[14] D. Lu, C. Xiong, Z. Zeng, and L. Lian, "A multimodal aerial underwater vehicle with extended endurance and capabilities," in *Proc. IEEE Int. Conf. Robot. Autom.*, May 2019, pp. 4674–4680.

[15] J. Zha, E. Thacher, J. Kroeger, S. A. Makiharju, and M. W. Mueller, "Towards breaching a still water surface with a miniature unmanned aerial underwater vehicle," in *Proc. Int. Conf. Unmanned Aircraft Syst.*, Jun. 2019, pp. 1178–1185.

[16] "Bell Boeing V-22 Osprey Fleet Surpasses 500,000 Flight Hours," 2019. [Online]. Available: https://boeing.mediaroom.com/2019-10-07-Bell-Boeing-V-22-Osprey-Fleet-Surpasses-500-000-Flight-Hours

[17] J. Judson, "V-280 Valor flies for the first time," *Defense News*, Dec. 2017. [Online]. Available: https://www.defensenews.com/breaking-news/2017/12/18/v-280-valor-flies/

[18] K. Wang, Y. Ke, S. Lai, K. Gong, Y. Tan, and B. M. Chen, "Model-based optimal auto-transition and control synthesis for tail-sitter UAV KH-Lion," in *Proc. 13th IEEE Int. Conf. Control Autom.*, Jul. 2017, pp. 541–547.

[19] J. E. Low, D. Sufiyan, L. S. T. Win, G. S. Soh, and S. Foong, "Design of a hybrid aerial robot with multi-mode structural efficiency and optimized mid-air transition," *Unmanned Syst.*, vol. 7, no. 4, pp. 195–213, Oct. 2019.

[20] L. Meier, D. Honegger, and M. Pollefeys, "PX4: A node-based multithreaded open source robotics framework for deeply embedded platforms," in *Proc. IEEE Int. Conf. Robot. Autom.*, May 2015, pp. 6235–6240.

Yu Herng Tan received the M.Eng degree in aeronautical engineering (with first class honours) from Imperial College London, London, U.K., in 2016. She is currently working toward the Ph.D. degree with the Unmanned Systems Research Group, the National University of Singapore.

Her research interests include unconventional aerial vehicles with multimodal locomotive capabilities.

Ben M. Chen (Fellow, IEEE) received the B.S. degree in mathematics and computer science from Xiamen University, Xiamen, China, 1983, the M.S. degree in electrical engineering from Gonzaga University, Spokane, Washington, 1988, and the Ph.D. degree in electrical and computer engineering from Washington State University, Pullman, WA, USA, 1991.

He is currently a Professor with the Department of Mechanical and Automation Engineering, The Chinese University of Hong Kong and a Professor with the Department of Electrical and Computer Engineering, National University of Singapore (NUS). He was a Provost's Chair Professor at NUS. His current research interests include unmanned systems, robust control, and control applications.

Dr. Chen is an IEEE Fellow. He has published more than 400 journal and conference articles and authored/co-authored 10 research monographs in systems and control theory, industrial applications, unmanned systems and financial market modeling. He had served on the editorial boards of several international journals including IEEE Transactions on Automatic Control and Automatica. He currently serves as an Editor-in-Chief of Unmanned Systems. He has received a number of research awards nationally and internationally. His research team has actively participated in international unmanned aerial vehicles competitions and won many championships in the contests.

Authorized licensed use limited to: National Univ of Defense Tech. Downloaded on February 24,2025 at 15:21:25 UTC from IEEE Xplore. Restrictions apply.